

Influence of the Flow Characteristics and Mud Physical Properties on the Performance of a Drilling Turbine

Khaled Sahnoune¹, Abderrahmane Benbrik¹, Ahmed S. Mansour², Mourad Moderres³

¹ *Laboratory of Petroleum Equipment Reliability and Materials, Faculty of Hydrocarbons and Chemistry, Université M'Hamed Bougara, Boumerdès, Algeria*

² *Mechanical Power Department, College of Engineering, Ain Shams University, Cairo, Egypt*

³ *Laboratory of Industrial Fluids, Measurements and Applications (FIMA) Science and Technology Institute, Khemis Miliana University, Algeria*

Received February 11, 2021; Accepted June 1, 2021

Abstract

For turbo drilling machine operations, several types of drilling mud can be used. The major factors influencing the choice of drilling fluid are: Cost, ecological impact, and the technical performance of the machine. Water-based drilling mud is widely used in drilling turbines. It consists of freshwater with additives such as sand. These added materials will influence the properties of the mud, increasing the density, and changing the rheological properties.

In this present work, the influence of the physical properties of the drilling mud (density, viscosity), and flow conditions (mass flow rate) on the performance and flow characteristics of a specified turbodrill Model is investigated. For this purpose, the computational fluid dynamics approach was used to simulate the flow inside one stage of the considered turbine. Various values of mass flow rate, density, and viscosity were tested. A very good agreement was found between the experimental measurements of the manufacturer and the current simulation results for the performance curves.

Keywords: *Turbodrill; CFD; Turbulence; Drilling mud; CFX; Performance analysis.*

1. Introduction

Turbodrills are all metal axial drilling machines, They can drill in a hard rock environment [1], in very deep wells where the pressure and temperature are very high. Therefore, these machines have a great importance in modern drilling technologies as directional drilling, and coil tubing. The reason of this renewed interest in this equipment is related to its high mechanical resistance, flexibility in using various types of drilling fluids and the compatibility with multiple models of the drill bit.

The working principle of the Turbodrill is to convert the hydraulic energy of the drilling mud into mechanical energy inside the turbine stage [2].

For turbo drilling machine operations, several types of drilling mud can be used. The main factors influencing the choice of the drilling fluid are [3] :

- Cost.
- Ecological impact.
- Technical performance of the machine.

Water-based drilling mud is widely used as the driving fluid of drilling turbines. Largely for economic reasons, the base fluid is freshwater with additives such as baryte or bentonite [4] . These added materials will influence the properties of the mud, increasing the density and changing the rheological properties especially the viscosity.

Studying the flow and the performance of turbodrills employing CFD simulations has been a subject of interest of recent researches. Many of them tested the physical properties of the mud and the flow condition on the performance of the Turbodrills. According to the extensive work of Monteiro *et al.* [5], a performance evaluation of a 200 stage drilling turbine was done

by using computational methods. Through the simulation, two different drilling fluid types were considered; seawater and brine. At different flow rates, the researchers investigated the changes of pressure contours, velocity vectors, output power, and other performance factors. As a result, optimum operation parameters are proposed for achieving the required rotational speed and torque for post-salt environments.

Yu Wang *et al.* [6] carried out an interesting study about small diameter Turbodrills, where a $\Phi 89$ blade was developed. The blade profile was imported into the software to create a numerical model of the single-stage blade. The multistage design of the turbodrill model was enabled by the optimization of the blade geometry. That optimization also helped in predicting the flow characteristics and performance. The obtained results showed that the turbodrill performance requirements can be achieved by their design. Furthermore, the prediction accuracy can be enhanced by the multistage model.

According to Zhang *et al.* [7], an optimization study on turbodrill blades was carried out. The researchers took the turbodrill tested on the bench as the case study. Using third-order Bezier curve fitting blade surfaces, the simulation model was built. An optimized design for the blades was proposed to obtain the new performance factors which gave an efficiency improvement of more than 10%.

Zhang *et al.* [8] prepared multiple cascade CFD models of turbodrill with different modified profile angles. The circumferential force and the hydraulic efficiency were chosen as the parameters of evaluation. Finally, the impact of the modified inlet and outlet flow angle on the turbine performance was analyzed. It was found that the slight modification of the outlet-flow angle might lead to turbine performance fluctuation. Therefore, the outlet-flow angle modification range was narrow and the modification value was small.

According to Wang *et al.* [9] a blade profile optimization was done based on a 3D model. A new blade geometry was obtained and was tested by CFD simulations. The influence of the fluid viscosity on the hydraulic performance was investigated. After that, a full turbodrill stage was fabricated, and experimentally tested on a bench.

Extensive studies on turbodrills were carried out [10-12]. Simulation tools were used to investigate the influence of the fluid type, flow rate, and the rotational speed on the machine performance, and the flow behavior represented by (velocity - pressure) contours inside the turbine. A structural analysis was conducted [10] to numerically calculate the deformation and stress distribution of the blade under the effect of the fluid flow.

In the current paper, we discuss the influence of some important factors on the turbodrill performance. The factors are the mass flow rate, density, and viscosity. For this task, ANSYS CFX 2020 R2 commercial package was used [11]. To simulate the flow inside one stage of the concerned turbine, the obtained simulation results were validated against the available experimental measurements for a specified model of the drilling turbine.

2. Preliminary analysis

2.1. Fluid flow inside one turbine stage

Before proceeding with the 3D simulations and the validation, key performance parameters have to be defined based on 1D mean line calculations and velocity triangles. Using the velocity triangles at the design operating conditions, performance factors such as power, torque, and hydraulic efficiency can be evaluated for the turbodrill. On the other hand, these factors can be measured experimentally, on the same realistic geometry of the turbodrill. The numerical results are compared, to the measurements.

The hydraulic power generated by each stage of the turbine [12]:

$$P_H = \rho \cdot \dot{m} \cdot U \cdot C_x (tg\beta_2 + tg\beta_3) \quad (1)$$

The output torque of one stage:

$$T = \rho \cdot \dot{m} \cdot r_m \cdot C_x (tg\beta_2 + tg\beta_3) \quad (2)$$

Hydraulic efficiency:

$$\eta_h = \frac{P_H}{\dot{m}\Delta p_{stage}} \quad (3)$$

2.2. Flow governing equations

The flow of water-based mud through the turbodrill stages is assumed to be isothermal and Newtonian with constant viscosity [21]. The continuous feeding of the turbine by this flow conserves a relatively constant temperature inside the turbodrill. In this case, the heat transfer effect is neglected and the energy equation is not considered in the current numerical study [13].

The flow inside hydraulic turbines is always fully turbulent. Hence, the flow field (velocity-pressure) is calculated based on Reynolds Averaged Navier-Stokes (RANS) equations. These equations are obtained by considering the time-averaged and fluctuation components: $u_i = \bar{u}_i + u'_i$; $p = \bar{p} + p'$

After taking the averaged equations into account, the following flow equations (in tensor notation) are obtained [13]:

$$\frac{\partial \bar{u}_j}{\partial x_j} = 0 \quad (4)$$

$$\rho \bar{u}_i \frac{\partial \bar{u}_j}{\partial x_j} + \rho \bar{f}_i = \frac{\partial \bar{p}}{\partial x_i} + \frac{\partial}{\partial x_j} \left(-\bar{p} \delta_{ij} + \mu \left(\frac{\partial \bar{u}_i}{\partial x_j} + \frac{\partial \bar{u}_j}{\partial x_i} \right) - \overline{\rho u'_i u'_j} \right) \quad (5)$$

In the current study, full turbulence k - ε two equations model is used to take the turbulence effects in the term $\overline{u'_i u'_j}$ into consideration [14]. The k - ε model of the transport equations are based on the turbulent kinematic energy k and the energy dissipation rate ε . The standard k - ε model, is based on the assumption that the flow is fully turbulent. More details on the governing equations and the turbulence modeling can be found in our previous work [13].

The rotating and stationary domains interacts during steady-state simulations through a so-called mixing plane interface. At the interface, the fluid region is divided into several circumferential bands. Within each band, the constant circumferential mean velocity and pressure are transferred from one domain to the other. This procedure is repeated at each iteration of the numerical computation. The non-slip condition (zero relative velocity) is applied to all walls. On the rotating domains, the stationary walls are modeled with an inverse rotational speed because the rotating domain remains static.

2.3. Geometry and mesh

In this work, only one model of turbodrill stage is considered. The geometry of the stator and the rotor are identical. Both have the same diameters of the hub and shroud that are 108 mm and 134 mm respectively. The blade height is 14 mm, the pitch of the stator and rotor is 22 mm, and the number of the blades is 30 for both [15].

The main difference between the stator and the rotor is that the latter is unshrouded and the blade orientation is inversed. The blade geometry specifications were got from the inventor patent [16] to build a full blade row by using ANSYS BLADEGEN software tool.

After building the geometric model, it had to be discretized to a large number of very small volumes for the Finite Volume Method (FVM) discretization method and CFD simulation. This process is performed with the ANSYS TurboGrid software which creates high-quality hexahedral meshes for turbomachinery. The quality of the CFD simulation highly depends on the quality of the mesh.

The numerical computation residuals tend to zero as the grid spacing and time step decrease. The reduction of residuals is known as the numerical convergence. Theoretically, the discretization error could be made arbitrarily small by gradual reductions in the time step and mesh element size. However, this requires increasing the memory size and the time of computation.

2.4. Simulation boundary conditions and assumptions

The numerical solution of the governing equations related to the fluid flow inside the considered drilling turbine needs some specifications for the domain external boundary conditions.

These specified boundary conditions should be sufficient to ensure a converged solution. All of the CFD simulations of this work as for the precedent work [13] were carried out by specifying a total pressure at the inlet and a mass flow rate at the outlet. The total pressure

at the inlet was set to 2000 psi (137.89 bars). The outlet mass flow rate for each simulation case varied. No-slip boundary condition was specified for the domain walls.

3. Results and discussion

3.1. Simulation methodology

The current numerical model was validated against experimental data in a previous paper [13]. In this work, more numerical results are compared to experimental results from the manufacturer of the machine model to further strengthen this numerical approach.

Several values of mass flow rate of the sludge were used while making its density constant (1196.82 kg/m³) and its viscosity (0.00089 Pa.s). For each value of the flow rate, the flow is simulated through the same geometry and same conditions described in the previous sections until convergence is reached. The residuals value was set to (RMS=10⁻⁶). The performance of the turbine is evaluated based on two values (power & torque). For each value of the rotor rotational speed, which was set to incrementally increase until the runaway value (zero torque) is reached, the values of the power and torque were calculated. Several values of mass flow rate were investigated at each speed of rotation. These values are as follows: 20, 24, 28, 33.97, 38, 42 and 46 kg/s respectively.

After plotting all power curves, the stall torque value was retained (for a zero rotational speed) and the maximum power as a function of the mass flow rate. The latter was compared to the experimental work that is available in the manufacturer's data of the Turbodrill specific model of the Turbodrill [15].

In the second part, several simulations were carried out for several values of the sludge density by fixing the mass flow rate (33.97 kg/s) and the viscosity (0.00089 Pa.s). For each density value, the same precedent procedure was used and the following values were considered: 1000, 1100, 1196.82, 1300, 1400, 1600 and 1800 kg/m³ respectively.

Finally, the effect of changing the fluid viscosity on the performance at the mass flow rate (33.97 kg/s) and density of 1196.82 kg/m³, the following values were considered: 0.001, 0.0015, 0.002 and 0.003 Pa.s respectively.

The influence of certain physical properties of the drilling mud is discussed. The effect of the density and viscosity on the performance of the axial turbine by estimating the power and torque is discussed. In addition to these parameters, the effect of the mass flow rate is also discussed. These three factors are the easiest to modify to control the operation of the drilling turbine as well as its performance.

3.2. Influence of mud density on power and torque

3.2.1. Power and torque curves

From Figure 1, it is noticed that all power curves have an inverted parabolic shape with a maximum value located at the half of the limit rotational speed (maximum power). The same observation can also be found in [5, 10]. It is also observed that the power values significantly increase with the increase of the mass flow rate of the sludge. Accordingly, if the mass flow rate is increased from 20 kg/s to 46 kg/s, the maximum power increases from 273 W to 3600 W, which is a considerable increase.

Table 1. Influence of the mass flow rate on performance and maximum torque

Mud mass flow rate (kg/s)	Stall torque (J)	Maximum power (W)
20	8.83449	273.615
24	12.9073	483.341
28	17.7539	779.53
34	26.3798	1422.35
38	32.7729	2072
42	40.7843	2723
46	49.1264	3606.92

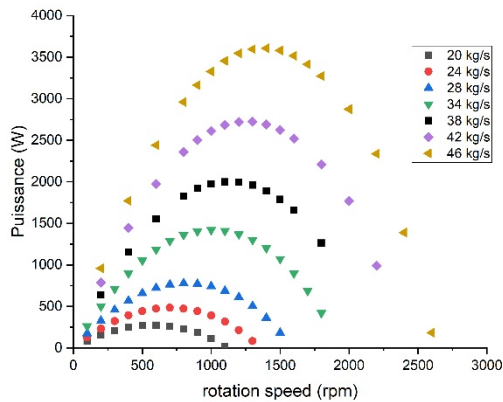


Figure 1. Power as a function of angular speed at different values of mass flow rate.

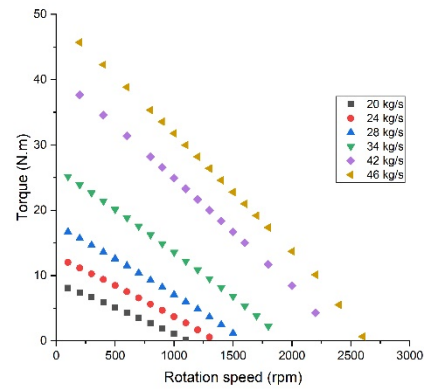


Figure 2. Torque as a function of speed of rotation for different mass flow rate values

Figure 2 shows the torque curves as a function of the rotational speed. It is noticed that they all have a decreasing linear shape. Starting from a maximum initial value at zero rotational speed (stall torque) to a zero value for the runaway speed. The torque values also increase in a very noticeable way. To give a good overview of the influence of the sludge mass flow rate on the performance, the Table 1 is presented.

This table shows that changing the mass flow rate leads to very significant changes when the power and torque are maximum. The obtained results give a very good agreement with the manufacturer's data [15].

Accordingly, it is concluded that to ensure a stable operational performance during drilling, a precise monitoring of the mass flow rate is necessary. Any slight change in the mass flow rate leads to large changes in the performance characteristics of the turbine, which negatively affects the drilling process.

3.2.2. Comparison between simulation and experimental values

The maximum power values shown in the previous table can be used to plot comparison curves between the results of the current numerical simulations and the experimental values of the turbodrill (model T122) [15]. Each point of the CFD simulation is obtained after doing tens of convergent simulations for a specified value of the mass flow rate and determining the maximum value of the power (see Figure 1) finally this is represented in the Figure 3.

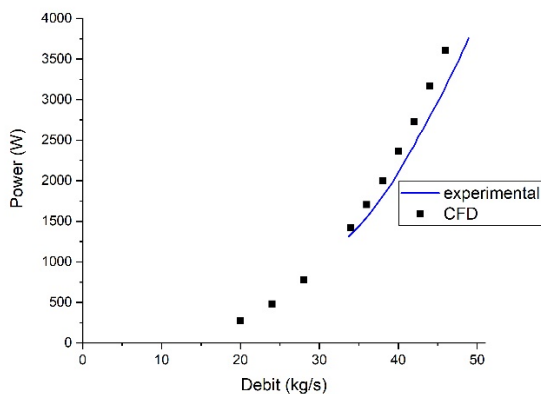


Figure 3. Comparison between numerical and experimental values of maximum power

Figure 3 shows a very good agreement between the numerical and experimental values. This shows the degree of accuracy of the current numerical simulations. Accordingly, more simulations were carried out to investigate the influence of the mass flow rate on the power generated by the turbine. This gives a wide range of numerical results which helps to understand more about the performance. The use of the chosen numerical approach allows a considerable reduction of cost and time to analyze the performance of the drilling turbines. This will be very beneficial on the design and manufacturing process of these machines.

3.2.3. Flow fields results

Figures 4, 5 illustrate respectively the distribution of velocity and pressure fields in the current simulated stage of a turbodrill for three respective values of the flow rate at maximum power condition (20 kg/s, 34 kg/s and 46 kg/s). The shape of the contours is very similar to that presented in previous studies [6, 13, 17].

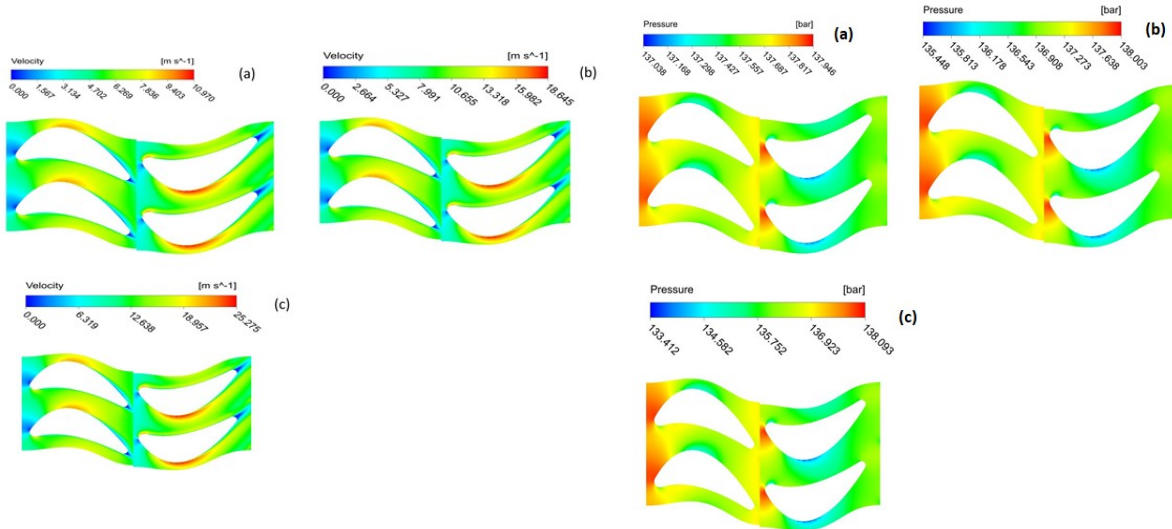


Figure 4. Velocity Fields (Mass flow rate **a:** $\dot{m}=20$ Kg/s ; **b:** $\dot{m}=34$ Kg/s; **c:** $\dot{m}=46$ Kg/s).

Figure 5. Pressure Fields (Mass flow rate **a:** $\dot{m}=20$ Kg/s ; **b:** $\dot{m}=34$ Kg/s; **c:** $\dot{m}=46$ Kg/s).

Changing the value of the mass flow rate does not change the general behavior of the flow fields. However, it has a great influence on the value of the velocity. On the other hand, the pressure did not change significantly. For example, it is noticed that the value of the maximum velocity in the velocity field increases from 10.97 to 25.275 m/s. This is expected due to the increase in the quantity of fluid passing through the same flow section (increase in flow rate).

3.3. Influence of mud density on the power and torque

3.3.1. Power and torque curves

It is observed that all the power curves have an inverted parabolic shape (Figure 6) with a maximum value located at the half of the limit speed [10]. Furthermore, it is observed that the power values significantly decrease with the increase in sludge density. The results indicate that an increase in the density from 1000 kg/m³ to 1600 kg/m³ is translated by a very noticeable decrease in the maximum power generated by the turbine from 2035 W to 795 W. This result can be explained by the increase in the inertia forces.

It is observed that all plots of the rotational speed versus the torque at different densities (Figure 7), have a linear decreasing behavior. Starting from a maximum initial value at zero rotation (stall torque) and ending at the runaway speed. It is also noticeable that the torque values significantly decrease with increasing the density. To understand the influence of mud mass flow rate on the performance, the following table is provided:

Table 2. Influence of density on maximum power and stall torque

Mud density (kg/m ³)	Stall (Torque (J))	Maximum power (W)
1000	31.6589	2035
1100	28.7442	1678.87
1200	26.3798	1422.35
1300	24.296	1200.7
1400	22.559	1035
1600	19.7794	796
1800	17.5905	630

The influence of the density on the maximum power is very important (Table 2). On the other hand, the effect of the density on the stall torque is noticed but to a lesser degree. For both maximum power and stall torque, they decrease when using denser mud fluid. This finding must be taken into account when choosing drilling fluids [2].

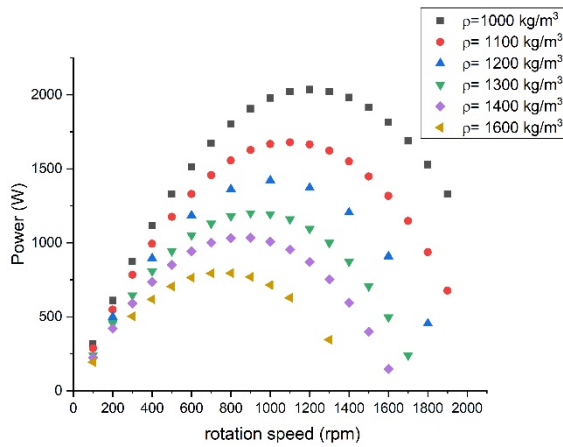


Figure 6. Influence of mud density on the generated power.

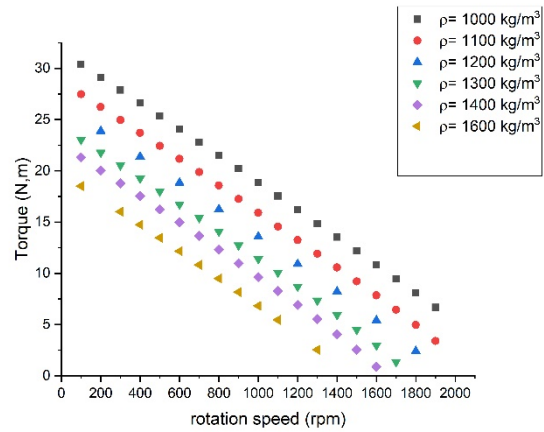


Figure 7. Influence of mud density on the turbine torque

3.3.2. Influence of the drilling mud density value on flow fields

The distribution of the velocity and pressure fields are presented in Figures 8 & 9 respectively. These contours are for a stage of the drilling turbine for three respective values of the density of the fluid (1000 kg/m³, 1200 kg/m³, 1400 kg/m³). They are simulated at the maximum power value.

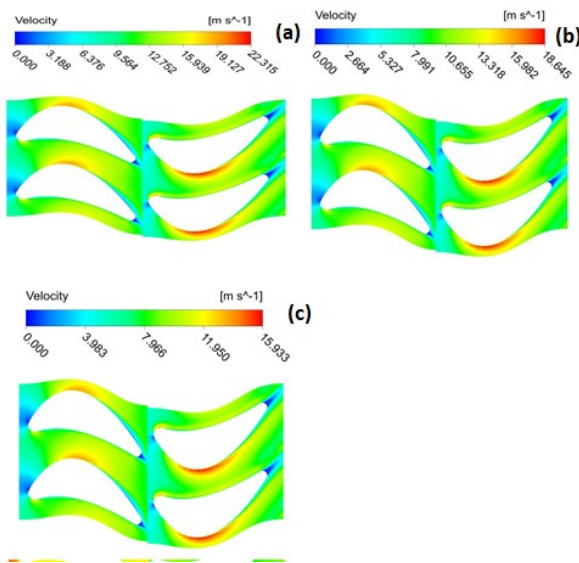


Figure 8. Velocity Field (a: $\rho=1000\text{kg/m}^3$; b: $\rho=1200\text{kg/m}^3$; c: $\rho=1400\text{kg/m}^3$)

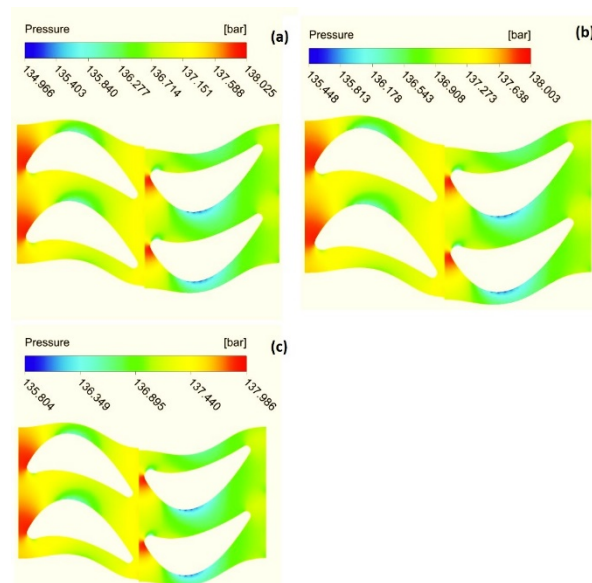


Figure 9. Pressure field (a: $\rho=1000\text{kg/m}^3$; b: $\rho=1200\text{kg/m}^3$; c: $\rho=1400\text{kg/m}^3$)

A significant decrease is observed in the value of the velocity (for the pressure, the change is not significant). For example, it is noticed that the value of the maximum velocity of the fluid in the turbine stage decreases from 22.315 m/s to 15.933 m/s. This occurs due to the increase of the fluid inertia forces by the increase in the fluid mass at a specific fluid volume. On the other hand, the pressure maximum value changed from 138.093 to 137.986 bars, which is a small change.

3.4. Influence of viscosity on turbodrill power

Figure 10 gives the power plots for several viscosity values ranging from 0.001 to 0.003 Pa.s. Unlike the flow rate and density, the influence of the drilling mud viscosity on the power values is not significant. When the viscosity increases, we notice a small decrease in power values. This can be attributed to the increase in frictional forces especially the drag on the rotor blades. Accordingly, this increases the losses in the turbine and decreases the generated torque and power.

Table 3. Influence of viscosity on maximum power and torque.

Mud viscosity (Pa.s)	Stall torque (J)	Maximum power (W)
0.001	26.464	1405
0.0015	25.85967	1349.07
0.002	25.37652	1305
0.003	24.5159	1245.22

We observe that the viscosity of the drilling mud has a least influence on performance (table 3). Power and torque slightly decrease when using a more viscous mud. However, this result must be taken into account to achieve the best-operating conditions for the turbodrill.

4. Conclusion

In this work, a parametric study of the influence of three important factors on the performance of a turbodrill was carried out. These factors are the mass flow rate, density, and viscosity. Numerical simulations were done to simulate the flow of mud inside one stage of the drilling turbine. After the convergence of the simulations, power and torque were calculated and the graphs of these outputs, were plotted as a function of the rotational speed of the rotor.

The results showed that the change of the mass flow rate of the used fluid produces very significant changes in the maximum power and torque. A very good agreement was also found between the numerical and experimental values of the maximum power generated by the turbine. This shows the good accuracy of the current numerical simulations.

The influence of the density on the maximum power and torque is very significant, but to a lesser degree, compared to the effect of the mass flow rate. It was also found that the maximum power and stall torque decrease if the density of the mud flow increases. The viscosity of the mud has the least influence on the turbine performance, it slightly decreases when using a more viscous mud.

The use of the current numerical approach allows a considerable reduction of cost and time to analyze the performance of drilling turbines that will be very beneficial on the design and manufacturing process of these machines.

Nomenclature

U	rotor velocity	α_i	absolute angles
C_x	absolute velocity axial component	β_i	relative angles
\vec{C}	absolute velocity	T	Torque
\vec{W}	relative velocity	P_H	Hydraulic power
U_i	Time averaged velocity	η_H	Hydraulic efficiency
u_i	fluctuation velocity	ρ	Mud density
Ω	rotational speed	\dot{m}	mass flow rate

Acknowledgment

This work was supported by a research grant (PRFU project: A05N01UN350120180002) from Direction Générale de la Recherche Scientifique et Développement Technologique (DGRSDT) (General Directorate of Scientific Research and Technological Development), Algeria.

References

- [1] Reich M, Picksak A, John W, Regener T. Competitive Performance Drilling with High-Speed Downhole Motors in Hard and Abrasive Formations. IADC/SPE Drilling Conference, February 23–25, 2000, New Orleans, Louisiana, ISBN: 978-1-55563-353-0.
- [2] Neyrfor Turbodrill Handbook, Schlumberger, Editor. 2012, Schlumberger Marketing Communications.
- [3] Radtke R, Glowka D, Rai M. High-Power Turbodrill and Drillbit for Drilling with Coiled Tubing. Oil & Natural Gas Technology, DOE Award No.: DE-FC26-06NT15486
- [4] Abbasi S, Fazlali A, Adimi M, Mohammadi AH. reparation of Hydrogels Based Methacrylamid by Thermal Method for Water Adsorption and Changing Rheological Properties of Bentonite-Base Drilling Mud. *Pet Coal*, 2020. 62(3): 754-764.
- [5] Monteiro VG, Tomita JT, Bringham C, Vastenavond A, Sampaio, Jr JHB. Performance Evaluation of a Hydraulic Turbine Used As a Turbodrill for Oil and Gas Applications in Post-Salt Environment. ASME Turbo Expo 2017: Turbomachinery Technical Conference and Exposition, Paper No: GT2017-63456, V009T27A012,
- [6] Wang Y, Xia B, Wang Zh, Wang L, and Zhou Q. Design and Output Performance Model of Turbodrill Blade Used in a Slim Borehole. *Energies*, 2016; 9(12): 1035.
- [7] Zhang X, Yu S, Gong Y, Li Y. Optimization design for turbodrill blades based on response surface method. *Advances in Mechanical Engineering*, 2016; 8(2): 1-12.
- [8] Zhang XD, Gong Y, Gou RY, Li JH, Wu JP, and Jiang ZJ. Modification and Analysis on Inlet and Outlet Angle of Turbodrill's Cascade Blade Profile. *Advanced Materials Research*, 2011; 317-319: 2126-32.
- [9] Yu W, Jianyi Y, Zhijun L. Design and development of turbodrill blade used in crystallized section. *Scientific World Journal*, 2014; 682963.
- [10] Mokaramian A, Rasouli V, Cavanaugh G. Fluid Flow Investigation through Small Turbodrill for Optimal Performance. *Mechanical Engineering Research*, 2013. 3(1).
- [11] ANSYS, I., ANSYS CFX-Solver Theory Guide, I. ANSYS, Editor. 2006, ANSYS, Inc.
- [12] Korpela SA. Principles of Turbomachinery. ed. I. John Wiley & Sons. 2020, ISBN-13: 978-0470536728.
- [13] Sahnoune K, Benbrik A, Mansour AS, Oussama R. Flow simulation and performance analysis of a drilling turbine. *Journal of Engineering Research*, 2020, 8(3): 256-270.
- [14] Sagol E, Reggio M, Ilinca A. ISRN Mechanical Engineering, Assessment of Two-Equation Turbulence Models and Validation of the Performance Characteristics of an Experimental Wind Turbine by CFD, 2012: Article ID 428671.
- [15] Neyrfor Turbodrill Handbook. ed. Schlumberger. 2012, Schlumberger Marketing
- [16] Natanael M, Nevlud KM, Beaton T, Beylotte J, Turbodrill with asymmetric stator and rotor vanes, US Patent, Smith International, Inc., p., 2008.
- [17] Mokaramian A, Rasouli V, Cavanaugh G. Turbodrill design and performance analysis. *Journal of Applied Fluid Mechanics*, 2015; 8(3): 377-90.

To whom correspondence should be addressed: Khaled Sahnoune, Laboratory of Petroleum Equipment Reliability and Materials, Faculty of Hydrocarbons and Chemistry, Université M'Hamed Bougara, Boumerdès, Algeria, E-mail: k.sahnoune@univ-boumerdes.dz